Growing spherulitic calcite grains in saline, hyperalkaline lakes: experimental evaluation of the effects of Mg-clays and organic acids

R. Mercedes-Martín[1], M.R. Rogerson[1], A.T. Brasier[2], H.B. Vonhof[3,] T. J. Prior[4], S. M. Fellows[4], J.J.G. Reijmer[3] Ian Billing[5], and H.M. Pedley[1]

1.Department of Geography, Environment and Earth Sciences, University of Hull, Cottingham Road, Hull, UK. HU6 7RX. E-mails: r.mercedes@hull.ac.uk; m.rogerson@hull.ac.uk

2. School of Geosciences, Meston Building, University of Aberdeen, Old Aberdeen, Scotland, UK. AB24 3UE

3: Faculty of Earth and Life Sciences, VU University Amsterdam, De Boelelaan 1085, 1081HV, Amsterdam, The Netherlands

4: Department of Chemistry, University of Hull, Cottingham Road, Hull, UK. HU6 7RX.

5: BP Exploration, Sunbury-on-Thames, United Kingdom.

ABSTRACT

The origin of spherical-radial calcite bodies – spherulites – in sublacustrine, hyperalkaline and saline systems is unclear, and therefore their palaeoenvironmental significance as allochems is disputed. Here, we experimentally investigate two hypotheses concerning the origin of spherulites. The first is that spherulites precipitate from solutions super-saturated with respect to magnesium-silicate clays, such as stevensite. The second is that spherulite precipitation happens in the presence of dissolved, organic acid molecules. In both cases, experiments were performed under sterile conditions using large batches of a synthetic and cell-free solution replicating waters found in hyperalkaline, saline lakes (such as Mono Lake, California). Our experimental results show that a highly alkaline and

highly saline solution supersaturated with respect to calcite (control solution) will precipitate euhedral to subhedral rhombic and trigonal bladed calcite crystals. The same solution supersaturated with respect to stevensite precipitates sheet-like stevensite crystals rather than a gel, and calcite precipitation is reduced by ~50% compared to the control solution, producing a mixture of patchy prismatic subhedral to euhedral, and minor needle-like, calcite crystals. Enhanced magnesium concentration in solution is the likely cause of decreased volumes of calcite precipitation, as this raised equilibrium ion activity ratio in the solution. On the other hand, when alginic acid was present then the result was widespread development of micron-size calcium carbonate spherulite bodies. With further growth time, but falling supersaturation, these spherules fused into botryoidal-topped crusts made of micron-size fibro-radial calcite crystals. We conclude that the simplest tested mechanism to deposit significant spherical-radial calcite bodies is to begin with a strongly supersaturated solution that contains specific but environmentally-common organic acids. Furthermore, we found that this morphology is not a universal consequence of having organic acids dissolved in the solution, but rather spherulite development requires specific binding behaviour. Finally, we found that the location of calcite precipitation was altered from the air : water interface to the surface of the glassware when organic acids were present, implying that *attached* calcite precipitates reflect precipitation via metal-organic intermediaries, rather than direct forcing via gas exchange.

Key words: Spherulite, hyperalkaline, stevensite, Mg-clays, organic acids, lacustrine

INTRODUCTION

Understanding the timing and growth mechanisms of unusual non-marine carbonate precipitates formed in sublacustrine environments is current focus for active geobiological and geochemical research (Della Porta, 2015; Wright and Barnett, 2015). A prominent feature of some sublacustrine sedimentary deposits are ≤ mm-sized spherulitic and radially divergent calcite allochems. These occur in abundance in the economically important Lower Cretaceous Pre-Salt basins of Brazil and Angola (Terra et al, 2010; Dorobek et al., 2012; Wright and Barnett, 2015), making them key "index allochems" for the environments recorded by these systems (Wright and Barnett, 2015). Spherulites are well known, and form in a wide range of carbonate environments, including soils (Chafetz and Butler, 1980; Verrecchia et al., 1995; Braissant et al., 2003), lakes (McGill et al., 1993; Wanas 2012; Bahniuk et a., 2015), hypersaline lagoons (Spadafora et al., 2010; Arp et al., 2012) and marine tidal-flat settings (Buczynski and Chafetz, 1993). However, a better understanding of the specific environmental conditions favourable for their formation can be gained through constrained laboratory experimentation.

In the geological record, spherulitic deposits were initially considered to be microbial laminites, forming 'oncoidal' to spherulite-rich layers that alternate with smectite layers (Luiz Dias, 1998; p.84). More recently focus has been on the possible abiotic catalysing role of co-occurring minerals in precipitating spherulitic calcite from solution (Wright and Barnett, 2015). Dorobek et al., (2012) suggested that spherical-radial components grew by displacive crystal growth mechanisms within previously deposited sediment. Particular emphasis has been given to specific substrates composed of hydrated magnesium clays, e.g. stevensite (Tosca and Wright, 2015; Wright and Barnett, 2015). These clays are

present in many modern lacustrine deposits and are also consistently found associated with the spherulites in the deposits of Brazilian Pre-Salt lakes (Luiz Dias, 1998; Terra et al., 2010; Tosca and Wright, 2015). This supports the suggestion that the paleo-lakes in question were both saline and highly alkaline (Calvo et al., 1999; Jones and Deocampo, 2003; Bristow and Milliken, 2011), as high salinity and high alkalinity (combined with high Mg/Si) are the conditions for authigenic precipitation of stevensite-like products (Tosca and Masterson, 2014). At the same time, Tosca and Wright (2015) suggested that the precipitation of Mg-clays (stevensite) from water would give rise to the formation of a poorly crystalline, viscous and extensively hydrated Mg-silicate gel, within which spherular carbonate could form. This is an important and novel hypothesis, meaning that deposits formed by these allochems are abiotic in origin. However, the tendency of stevensite to precipitate as a gel, and the capacity of solutions supersaturated with stevensite (as would be required to maintain the gel) to promote voluminous calcite precipitation with unusual spherulitic morphologies, both require testing.

Organic acids as catalysts of spherulite growth?

The nucleation patterns and crystallization processes of carbonate precipitates, including spherulites, are well described in environmental and materials science literature (i.e., Buczynski and Chafetz, 1993; Verrecchia et al., 1995; Tracey et al., 1998a,b; Braissant et al., 2003; Aloisi et al., 2006; Rodriguez-Navarro et al., 2007; Sánchez-Navas et al., 2009; Tourney and Ngwenya, 2009; Andreassen et al. 2010; Beck and Andreassen, 2010; Ercole et al., 2012; Sánchez-Navas et al., 2013). Many additives to aqueous solution have been found to promote spherulite formation, and these include oxygen-rich organic acid molecules, such as citric or malic acids (Meldrum and Hyde, 2001), or aspartic acid

(Braissant et al., 2003; Wolthers et al., 2008). Although some studies have focussed on the impact of these substances in the spherulitic growth of metazoan calcitic skeletons (Kim et al., 2011), organic acid molecules are known to be a major component of microbial extra-cellular polymeric saccarides (EPS) (Dittrich and Sibler, 2010), and so are freely available in sites of lacustrine authigenic carbonate formation. Building on pioneering work on the role of benthic biofilms in regulating where precipitation occurs (Arp et al., 1999; Pedley, 1994), recent studies demonstrate the capability of extracellular polymeric substances as active catalysts in the mineralisation process (Rogerson et al., 2010; Rogerson et al., 2008). Their influence has been shown to be sufficient to help overcome otherwise limiting kinetic barriers to precipitation of less favoured components like Mg-rich dolomite (Krause et al., 2012) and to provide the first-order control on trace element incorporation into low Mg-calcite (Saunders et al., 2014). Micron-size spherical-radial calcite has been recognised as an apparently universal consequence of precipitation within biofilms, demonstrated by controlled laboratory and field investigations (Pedley et al., 2009). Consequently, involvement of organic materials appears to present a viable counter-hypothesis to stevensite-gel catalysis for the formation of calcitic spherulitic grains in alkaline and saline lakes (*sensu* Tosca and Wright, 2015).

Alginic acid provides a documented case study of dissolved organic molecules that alter the crystallography of calcite (PerryIV et al., 2006). It is one of the uronic acids, a group which make up 20 – 50% of the polysaccharides produced in a wide range of EPS (Christensen and Characklis, 1990; Saiz-Jiménez, 1999), generated by marine and terrestrial bacteria (Kennedy and Sutherland, 1987). Alginic acid is common polymer produced by microbial taxa (e.g. *Azotobacter vinelandii* and *Pseudomonas aeruginosa*

(Boyd and Chakrabarty, 1995), which are ubiquitous in modern (Hardalo and Edberg, 1997), and presumably palaeo-lake waters. As a hydrophyllic polyuronic acid it is very soluble and has an excellent potential to form colloids (PerryIV et al., 2006). Most importantly here, alginic acid has been shown to actively influence the growth and morphology of calcite crystals by selectively binding onto specific crystal planes, primarily the $(10\bar{1}4)$ cleavage plane (PerryIV et al., 2006). It has been shown to bind to specific calcite crystal step-edges, disrupting the crystal structure and impeding continued growth (Orme et al., 2001). This mechanism is widely reported in the materials chemistry literature, but the consequences of step-edge binding are dependent on other environmental conditions such as pH, ionic strength and solution composition and therefore are difficult to predict in nature.

Experimental study of spherulite nucleation and growth

Here, we investigate the two hypotheses described above using constrained laboratory experiments. Specifically, we investigated 1) whether supersaturation of a lake-like water fluid with stevensite influenced calcite precipitation rate; whether this mineral precipitated as a gel in these chemical circumstances; and whether calcite precipitated in these conditions naturally formed spherulitic grains; 2) whether organic acids impacted on precipitation rate and precipitation morphology; and 3) whether alginic acid and other environmentally common organic molecules produced similar results. Experiments were performed in sterile conditions in order to eliminate metabolic and unknown metabolite influences, and control experiments were undertaken using only the 'lake-like waters' to demonstrate precipitate types and morphologies in the absence of all additives.

MATERIAL AND METHODS

Synthetic experimental solutions designed to be similar to Mono Lake waters in California (Connell and Dreiss, 1995), except with high super-saturation with respect to $CaCO_3$ phases (composition in Table 1), were produced in iterative 1 litre batches. Calcite deposits were grown from aliquots of these solutions in batch experiments with 4 replicates contained in 100ml conical glass flasks, sealed by air-permeable but microbe-impermeable foam bungs. All experiments were performed under complete sterility. To achieve this, powdered chemicals and glass wear were heat-sterilised by autoclave at 160^{o}C for 2 hours. Items that could not be heat-sterilised (plastic pipette tips and tubes) were treated with 16% hydrogen peroxide solution overnight. After preparation of solution batches, water was passed through sterile 20μm filters to remove any biological contamination that may have occurred subsequent to autoclaving and also to remove any precipitates that occurred during solution preparation. Precipitates were analysed from autoclaved, frosted glass slides placed into the flasks before addition of the solution. Once the solution had been added and they were sealed, the flasks were agitated by a tipping flask shaker to ensure their contents remained well mixed. Experiments were maintained for 24 or 45 days at 25^{o}C.

In addition to control batches (experiments hereafter designated X), four experimental treatments were investigated using the same standard solution with the addition of: 1 mg L^{-1} alginic acid (a component of EPS) (experiments hereafter referred to as AY); 1 mg L^{-1} stevensite (experiments hereafter referred to as S); 1 mg L^{-1} sodium carboxymethil cellulose (a component of Transparent Extracellular Polymers (experiments hereafter

referred to as T); Passow, 2002); 1 mg L^{-1} alginic acid and 1 mg L^{-1} stevensite (experiments hereafter referred to as SAY). After each experiment terminated, pH was measured, the solution was sampled and the frosted slides were autoclaved at 105°C. Within 1 hour the slides were carbon coated and observed with a Zeiss EVO60 Scanning Electron Microscope (SEM). Friable crystals accumulated in the bottom of the flasks were also collected and analysed using the same SEM. Elemental x-ray analyses were also performed in this study with an Inca System350 Energy Dispersive X-ray Spectrometer (EDX).

X-ray powder diffraction data were collected from ground samples mounted in stainless steel sample holders. A PANAlytical Empyrean diffractometer operating in Bragg-Brentano geometry with copper $K\alpha_1$ (λ = 1.540546 Å) and a PIXEL detector was used for the data collection. Where samples were attached to the surface of glass slides, these slides were mounted directly on the instrument.

A pure Mg-stevensite composition was used in these experiments to be as close as Tosca and Wright (2015) model (the ideal composition being $(Ca_{1/2}Na)_{1/3}Mg_3Si_4O_{10}(OH)_2.4H_2O$)). This material was synthesised without the need for hydrothermal conditions using a procedure adapted from Sychev et al., (2000). This was as follows. To make approximately 10g of stevensite (quantitative yield after drying) were used the following masses: 5.08g of fumed silica, 15.25g of urea, 0.83g of $Ca(NO_3)_2.4H_2O$, 0.60g of $NaNO_3$, 16.293g of $Mg(NO_3)_2.6H_2O$. Fumed silica in 200 ml deionized water was boiled under reflux for about 1hr. To this were added all of the metal salts dissolved in a further 50 ml deionized water. This mixture was then refluxed gently with stirring (~95 °C) for 65 hrs prior to addition of urea. This mixture was refluxed for a further 55 hrs and then allowed

to cool to room temperature and filtered. The solid product was subsequently dried at ~95 °C for 24 hours. The X-ray powder diffraction pattern for the resulting stevensite can be found in Supplementary Figure 1.

Mg, Ca and Si in aqueous solution samples were measured using a Perkin Elmer Optima 5300DV inductively coupled optical emission spectrometer (ICP-OES). The selection of the analytical lines used in the results was based on the Perkin Elmer recommendations for the Optima 5300DV spectrometer, 393.366 nm for calcium, 280.271 nm for magnesium and 251.611 nm for silicon. Calibration standards were prepared using 1000 ppm standard stock solutions (99.9% pure or greater, PrimAg, Xtra, Romil, Cambridge) of calcium and magnesium. Samples for analysis were diluted with 5% ultrapure HNO_3 to bring the expected concentrations to within or very near the linear calibration of the standards.

Alkalinity was measured using a Mettler-Toledo T50 digital titrator using a DGi117-water pH electrode and a Rondolino autosampler.

EXPERIMENTAL RESULTS

Crystals precipitated in the control experiment (X)

Calcite in the control experiment precipitated as subhedral to euhedral crystals (Fig. 1A and B). Composite forms include spherulite-like particles constituted by well-defined rhombic and trigonal bladed calcite crystals, the edges of which are smooth and tend to form imbricated twin clusters up to 20µm in diameter (Fig. 1A asterisk and 1B). Some scattered euhedral rhombohedral and prismatic calcite crystals (up to 20µm diameter) are also observed (Fig. 1A, top left). Abundant subhedral to euhedral cubic crystals of

halite with diameters less than 5µm were recognised (Na in Fig. 1C), along with patches of halite crusts developing chevron overgrowth crystals (Fig. 1 D). Calcium concentrations of the solution decreased during the experiment (see below), but development of crystals on the glass slides was comparatively limited, suggesting that substantial precipitation had occurred elsewhere. Visual inspection indicated that this additional precipitation took place at the air-water interface in the neck of the flask.

========== FIGURE 1 HEREABOUT ==========

Crystals precipitated in the presence of alginates (AY)

A second batch of flasks was prepared by the addition of 1 mg of alginic acid to aliquots of the synthetic "lake water" solution to investigate any catalytic effects of the alginic acid on calcite growth. In this experiment, specific crystal morphologies were found after 24, 37 and 44 days. First, spheroidal clusters of imbricated rhombohedron twins (up to 10µm diameter each; Figs. 2A, and 2B) displaying hollow centres (Fig. 2C) were nucleated within the first 24 days. The identity of these precipitates has been confirmed as calcite by X-ray powder diffraction (Fig. 3), and their clusters seemed to grow by forming dispersed spherulitic aggregates (up to 40µm diameter) which then fused together to generate a well-defined agglomeration of spherules (spherulitic crusts) as observed after 37 days (Fig. 2B). Once the first layer of spherules had formed, newer calcium carbonate precipitates nucleated above the previous crystals, giving rise to distinctive botryoidal crusts,

hundreds of µm in length, which were composed of subhedral to euhedral crystals with rhombohedral to prismatic shapes, as seen after 44 days in Fig. 2D.

========== FIGURE 2 HEREABOUT ==========

========== FIGURE 3 HEREABOUT ==========

Crystals precipitated in the presence of sodium carboxymethil cellulose (T)

Experiments carried out by the addition of 1 mg of sodium carboxymethil cellulose to the synthetic "lake water" solution gave rise to the nucleation of distinctive calcium carbonate precipitates after 26 days (Fig. 4). Sheets of tiny (5 to 10 µm in length) well-formed euhedral calcite rhombohedra were formed (Fig. 4A, B). Common inter-grown twinning between calcite rhombohedra were observed. In some cases, up to 40 µm-length thin calcite crusts were attached to the previously formed calcite rhombohedra. These crusts were composed of nanometre-thick spheroidal calcite aggregates that eventually built up to 10µm diameter hollow spherical coatings of calcite (Fig. 4C). In addition, calcite crusts also evolved into numerous individual and slightly elongated hollow spheres, each up to 3 µm in diameter. These spheres could form cluster aggregates and were found intermingled with calcite rhombohedra (Fig. 4D).

========== FIGURE 4 HEREABOUT ==========

Crystals precipitated in presence of stevensite (S)

In an experiment with stevensite added to the synthetic “lake water”, patchy and individual prismatic subhedral to euhedral calcium carbonate crystals up to 20 µm length were nucleated. Calcite crystals were commonly needle shaped, and sheet-like elongated rhombohedral bouquets that were up to 30µm length also formed after 25 days (Cal in Fig. 5A, B). Calcium carbonate products of this experiment commonly exhibited inter-grown twinning (arrow in Fig. 5A). In addition, subhedral to euhedral sheet-like stevensite crystals (up to 50µm diameter) precipitated from the solution, and were found intermingled with calcite crystals (St in Fig. 5A to C). These stevensite crystals were distinct from abundant macroscopic (mm-sized) stevensite crystals that were collected from the bottom of the flasks. The latter crystals displayed smoothly curved concentric rings through conchoidal faces, and were interpreted as relict grains of the clay added at the start of the experiment (Fig. 5D). No evidence for stevensite gel formation was observed.

========== FIGURE 5 HEREABOUT ==========

Crystals precipitated in the presence of stevensite and alginates (SAY)

The addition of stevensite and alginates to synthetic “lake water” resulted in calcium carbonate precipitates that were scarce and limited to tiny (up to 5 µm diameter) anhedral aggregates, and very occasionally, subhedral prismatic forms (up to 10 µm length) (Cal in Fig. 6A) after 24 and 37 days incubation. In addition, abundant hydrated

Mg-clay crystals nucleated in the form of dispersed and small anhedral aggregates (up to 15µm diameter; EDX in Fig. 6B and St in Fig. 6C). Subhedral cubic to rhombohedral aggregates of sodium chloride crystals with diameters less than 5µm were also produced (Na in Fig. 6B and C). As in the "S" experiment described above, abundant mm-sized stevensite crystals were also found having accumulated in the bottom of the flasks (Fig. 6D), yet no evidence for stevensite gel formation was detected.

========== FIGURE 6 HEREABOUT ==========

Hydrochemical parameters

Within the Control (X) and alginate (AY) flasks, more than 90% of the calcium was lost from solution during the experiment. In the presence of stevensite, this calcium loss was reduced by approximately half after 45 days (Table 1), indicating that a substantially reduced mass of precipitate developed.

========== TABLE 1 HEREABOUT ==========

Precipitation rate of $CaCO_3$ can be calculated from the mass balance of calcium in solution. All experiments showed an inverse power deceleration of precipitation rate, which is consistent with the solution consuming its supply of calcium and carbonate and thus developing sequentially lower saturation indices. This progressive decrease in dissolved

calcium concentrations and lowering of solution calcite saturation limited the length of time experiments could be run for, and also means that the last formed crystals were potentially formed under different saturation conditions to those that produced the first crystals in each batch. Calcium loss from solution was initially similar in the control and stevensite experiments, whereas higher rates of Ca loss were found in the presence of alginic acid, and lower rates in the stevensite + alginic, and TEP experiments (Fig. 7). Precipitation rate rapidly slowed in both experiments where stevensite was present, indicating that these flasks approached equilibration earlier, and at a higher calcium concentration. This is reflected in the relative lack of total calcite precipitate developed in these synthetic environmental conditions. After 24 days, the alginic acid experiment reduced its precipitation rate to slightly less than the control experiment, and after 45 days produced marginally less precipitate.

The initial synthetic "lake water" solution had 300 mg L^{-1} of magnesium, but where stevensite was added, substantial Mg was gained by the solution during the experiment (Fig. 8). That Mg/Si phases were supersaturated in these flasks was demonstrated by new precipitates being found on the glass slides (see above). Similarly, additional silicon was found in the stevensite-bearing flasks at the end of the experiments (Fig. 9). Where stevensite was present, this constituted the primary source of dissolved Si: otherwise, silicon addition came from minor dissolution of the glass by the relatively high pH solution at the start of the experiment.

========== FIGURE 7 HEREABOUT ==========

========== FIGURE 8 HEREABOUT ==========

========== FIGURE 9 HEREABOUT ==========

DISCUSSION

The experiments reveal that spherulitic-radial calcite will grow within saline, alkaline water in the presence of specific dissolved organic acids. This supports the hypotheses for the origins of ancient lacustrine spherulitic grains that invoke microbial activity. We emphasise that the experimental system developed here was completely sterile, the solution was not sufficiently concentrated to form a gel, and that the analogous organic acids will have been present in any solution in which microbes produced extracellular polymeric substances. As dissolved organic molecules can move away from the cells producing them by diffusion and advection, there is no need for localised microbial activity for this mechanism to operate in a lake. Microbial communities are both abundant and productive in modern lakes such as Mono Lake, California (Humayoun et al., 2003), Lake Van, Turkey (Lopez-Garcia et al., 2005), and the Kenyan and Tanzanian Rift Valley Lakes (Jones and Renaut, 1995, 1998; Rees et al., 2004; Renaut et al., 2013). It is therefore very likely that the simulated conditions will have been satisfied in most if not all Phanerozoic alkaline lakes, making the presence of organic acids in solution arguably the simplest means of producing spherulite carbonate deposits in such environments.

The size of the spherulites grown in the experiment (up to 20 μm) is smaller than the size of the grains noted in the Pre-Salt lacustrine deposits of the South Atlantic (mm sized, Wright and Barnett, 2015). This probably reflects the small volume of solution used in the

experiment, limiting the duration the growing allochem was exposed to supersaturated water. The saturation index of the water would have fallen rapidly during the experiment, from the initial 1.65 (calculation of saturation index done according to (Rogerson et al., 2014)). These grains were therefore denied the opportunity to grow to larger size, and the difference to the Pre-Salt allochems is likely a scaling issue. It should further be noted that both in the alginic acid and in the sodium carboxymethil cellulose experiment, precipitate morphology changed after 37 and 26 days, respectively (Fig. 2c and Fig. 2d). This change in precipitate morphology coincided with falling calcite saturation of the solutions, and in the alginic acid experiment this resulted in the development of botryoidal crust fabrics. We infer that calcitic botryoidal crust growth may have developed under conditions highly analogous to those of the Pre-Salt spherical-radial calcite, although with slightly lower calcite supersaturation.

Comparison of Figures 2 and 4 to Figure 1 show that the coverage of calcite on the frosted glass slides was far greater in the presence of both alginic acid and carboxymethil cellulose than in the control experiment. We thus infer that the physical location of crystallisation was altered by the presence of extracellular polymers, causing calcite nucleation to preferentially take place *attached* to the glass slide, rather than taking place in the water column and then settled *loosely* in the bottom of the flasks (B. Jones Pers. Comm., Bonny and Jones, 2003; Jones and Peng, 2014). This has previously been found in experiments under karst-like waters in flowing systems (Pedley et al., 2009; Rogerson et al., 2008). Confirmation of this earlier finding indicates that this translation of mineralisation sites is persistent and related to the presence of the organic acids within EPS, and not the proximity of microbial metabolisms here. A key consequence of this observation is that although in the control case, mineral formation primarily reflects gas

exchange at the air-water interface, this is not the normal case for systems where organic acids are involved in mineral formation. Moreover, the sterile conditions used for our experiments here demonstrate that this process is independent of metabolic processes that take place within benthic biofilms.

Influence of stevensite (and Mg) on the precipitation of $CaCO_3$

Supersaturating the solution with respect to stevensite clay did not alter the morphology of calcite precipitates, but rather significantly reduced the rate of calcite formation after the first 24 days. This experiment does not discount the possibility that carbonate spherulites may grow in Mg-Si gels; indeed this is well attested in the chemical engineering literature where such gels were exposed to a mixing interface between calcium chloride and sodium carbonate solutions (Beck and Andreassen, 2010). However, it does call into question whether voluminous spherulitic calcite grains were likely to have developed in Phanerozoic alkaline lakes. Firstly, our solution did not form a gel, and the controls on gel formation are as yet unclear. Moreover, to achieve the very high rate of precipitation typical of spherical-radial crystal growth (Sunagawa, 2005), saturation of the solution within the gel would need to be considerably enhanced beyond the condition of the solution used in this experiment. The synthetic “lake water” solution we used was more saturated than modern Mono Lake water, and therefore at the upper limit of supersaturation known in modern natural systems (Rogerson et al., 2014). A spherulite producing solution in an ancient setting may have required saturation with mixtures of $CaCl_{2(aq)}$ and $Na_2CO_{3(aq)}$, as used in chemical engineering systems (Beck and Andreassen, 2010) but the geological record suggests this is perhaps more unlikely than stevensite saturation in the natural world. Further doubts about the requirement for stevensite

saturation to produce spherulites are raised by the observation that addition of alginic acid to the solution supersaturated with stevensite impeded calcite growth still further, and did not result in spherulitic calcite morphologies (Fig. 6).

The negative impact of stevensite addition to the system probably reflects the inhibitive nature of magnesium (enhanced in stevensite-containing experiments; Fig. 10) on calcite precipitation. The inhibition of calcite formation in the presence of raised Mg concentration is long established (Folk, 1974) and is beginning to be quantified empirically (Niedermayr et al., 2013). The result we present is therefore not unexpected, but a predictable limitation on the ability of supersaturated Mg-phases to promote calcite precipitation.

Role of organic acids in controlling crystal growth

Based on the presented empirical evidence, the impact of alginic acid binding onto the $(10\bar{1}4)$ surface of the calcite crystal is to promote radial growth, resulting in a tendency for alginic acid-bearing solutions to produce calcite with spherical morphologies. Given previous findings of similar morphological consequences of organic acid addition to calcite-mineralising systems (Braissant et al., 2003), we suggest that high calcite supersaturation is also an important condition promoting spherical-radial growth. It is probably the scarcity of environments where calcite is precipitated sufficiently rapidly that results in these allochems being comparatively rare, rather than any lack of presence of organic acids. This behaviour does seem to be specific to organic acids, as it is not found in the experiment where carboxymethil cellulose was added. There may well be an additional control on spherulite distribution related to the specific organisms producing organic acids in any given setting.

A secondary, but equally important, empirical finding of this experiment is that far more of the fact that calcite was formed in the experiments where organic molecules were added, calcite nucleation took place *attached* to a substrate whereas in experiments lacking organic molecules this was not frequent. This was the case for both alginic acid and carboxymethil cellulose. Indeed, in some of the control experiments the $CaCO_3$ on the frosted slide was so sparse that no XRD record of it could be found, despite the solution mass balance showing that these experiments had more precipitation of these phases than the organic acid experiments (Fig 7). This means that the specific mechanism of mineral formation is different in the presence of the extracellular polymers than it is without. We suggest that the high surface area of the glass slide provided binding sites for charged organic acid molecules in solution (uronic acids are known to show strong binding with silicon ions (Schwarz, 1973)), which then provided a substrate onto which solid $CaCO_3$ formed, in close analogy to the mechanism suggested by Saunders et al., (2014). Metal-organic precursors to calcite are well-known to materials chemists (Kim et al., 2011) and the $CaCO_3$ has been found to initially form as an amorphous phase. Logically, this means that mineralisation in the presence of organic acids is not occurring as a *direct* consequence of gas exchange at the air-water interface. Equally, it means that rooted crystals found ubiquitously in nature (B. Jones Pers. Comm., 2015) also do not form as a *direct* consequence of gas exchange. This observation has major consequences for our understanding of mineralisation of calcite within natural systems with biofilms, as the direct linkage of mineralisation and gas exchange is an underlying assumption in the geological interpretation of almost all terrestrial carbonate mineral forming systems (Rogerson et al., 2014).

Implications for environmental interpretation of spherulite facies

While our experiments do not disprove that stevensite gels *can* form spherular-radial calcite, they do show that they can be straightforwardly formed by the types of solution expected in these alkaline, saline lakes so long as environmentally common organic acids are present in solution. This presents a very simple mechanism for the development of voluminous spherulite facies, and therefore we recommend that a colloidal organic control is considered when geological spherulite deposits are interpreted. The strong negative impact of the raised magnesium in solution needed to maintain active precipitation of stevensite further emphasises that this mechanism is less likely than an organic mechanism. The failure of our solutions to produce gels also indicates that more needs to be understood about the clay-catalysis mechanism.

As spherulites seem likely to be a consequence of organic acid intervention in the crystal growth mechanism, and as different organic acids result in different grain morphologies, it is logical to conclude that microbial activity provides a major key to the development of carbonate spherulitic grains. These facies should be considered microbial-influenced facies *sensu lato*. The lack of direct observation of conventional calcified microbial features is compatible with the exclusion of metabolic effects produced by endolithic or mat-forming organisms. Lack of entombed microorganisms may simply indicate limited microbial activity at the site of deposition. Neither of these conditions limits the hypothesis presented here, as the majority of EPS produced in a lacustrine system comes from planktonic photosynthetic communities, and settles through the water column to the bottom as transparent extracellular polymers (TEP) (Passow et al., 2001; Passow, 2002a, b; Bhaskar and Bhosle, 2005). Organic acids found in lake-bottom water can therefore be a product of planktonic exudation from surface water, regardless of the activity of benthic microbial systems. Further work is needed to fully understand the

microbial ecology and exudation processes of specific molecules within the system, and this promises to be a fruitful direction for future research.

Recent report of Mg-Si phases growing within biofilm masses (Burne et al., 2014), potentially even as precursors to $CaCO_3$ phases, provides a further perspective on the relationship of these two minerals. The observation from Lake Clifton that Mg-Si and $CaCO_3$ phases are spatially and temporally separate is compatible with our experimental finding that the enhanced Mg concentration needed to precipitate minerals like stevensite impedes calcite formation. Equally, the conclusion of Burne et al. (2014) that in these settings both Mg-Si and carbonate phases must be assumed to be "microbialites" appears to be a good basis for further investigation.

CONCLUSIONS

Radial-spherular calcite will grow straightforwardly within saline, alkaline waters in the presence of specific environmentally-common organic acids (in this case, alginic acid). This occurs due to the binding of this molecule onto the step-edge of the growing crystal. Despite this being a crystal inhibition process, the rate of precipitation is only marginally reduced. The presence of this molecule (and other organic polymers, in this case carboxymethil cellulose) also results in an increase in the precipitation at the sediment-water interface, which is probably a result of the organic molecules binding onto the surface, and providing a template for mineral precipitation. This indicates that gas exchange does not directly control mineralisation when calcite is produced via metal-organic intermediaries.

The same synthetic "lake water" saline, alkaline solution produced crystalline precipitates rather than a gel when supersaturated with stevensite. Due to the inhibitory effect of

raising the magnesium concentration, calcite precipitation rate was reduced by ~50% in this experiment and the carbonate mineral products were subhedral calcite crystals similar to the control experiment.

We conclude that spherulitic growth of calcium carbonate is likely to have formed extensively at the sediment-water interface in Phanerozoic alkaline lakes that held organic acids in solution, while clay-gels are not required to form voluminous deposits of spherulitic grains in Phanerozoic lacustrine environments.

ACKNOWLEDGEMENTS

BP Exploration Co. is thanked for funding, and particularly the Carbonate Team (Anna Matthews, Teresa Sabato Ceraldi, and Darryl G. Green) for supporting this research and for fruitful discussions. Mark Anderson, Kim Rosewell, and Tony Sinclair (University of Hull) are thanked for laboratory assistance, and for SEM sample preparation and set-up respectively. The technical and human support from Prof. Jörg Hardege and Maggy A. Harley (University of Hull) was key to perform these experiments. We would like to acknowledge an anonymous reviewer for the detailed and constructive comments, and Brian Jones's editorial handling of the manuscript which is greatly appreciated.

REFERENCES

Aloisi, G., Gloter, A., Krüger., Wallmann, K., Guyot, F., Zuddas, P. (2006). Nucleation of calcium carbonate on bacterial nanoglobules. Geology, 34, (12), 1017-1020.

Andreassen, J-P., Flaten, E. M., Beck, R., Lewis, A. E. (2010). Investigation of spherulitic growth in industrial crystallization. Chemical Engineering Research and Design, 88, 1163-1168.

Arp, G., Thiel, V., Reimer, A., Michaelis, W. and Reitner, J. (1999) Biofilm exopolymers control microbialite formation at thermal springs discharging into the alkaline Pyramid Lake, Nevada, USA. Sedimentary Geology 126, 159-176.

Arp, G., Helms, G., Karlinska, K., Schumann, G., Reimer, A., Reitner, J., Trichet, J. (2012). Photosynthesis versus exopolymer degradation in the formation of microbialites on the atoll of Kirimati, Republic of Kiribati, Central Pacific. Geomicrobiology Journal, 29, 29-65.

Bahniuk, A. M., Anjos, S., França, A. B., Matsuda, N., Eiler, J., McKenzie, J. A., Vasconcelos, C. 2015. Development of microbial carbonates in the Lower Cretaceous Codo Formation (north-east Brazil): implications for the interpretation of microbialite facies associations and palaeoenvironmental conditions. Sedimentology, 62, 155-181.

Beck, R., Andreassen, J-P. (2010). Spherulitic growth of calcium carbonate. Crystal Growth and Design, 10, 2934-2947.

Bhaskar, P. V., Bhosle, N. B. (2005). Microbial extracellular polymeric substances in marine biogeochemical processes. Current Science, 88, (1), 45-53.

Bonny, S. and Jones, B. (2003) Microbes and mineral precipitation, Miette Hot Springs, Jasper National Park, Alberta, Canada. Canadian Journal of Earth Sciences 40, 1483-1500.

Boyd, A. and Chakrabarty, A.M. (1995) Pseudomonas aeruginosa biofilms: role of the alginate exopolysaccharide. Journal of Industrial Microbiology 15, 162-168.

Braissant, O., Cailleau, G., Dupraz, C. and Verrecchia, E.P. (2003) Bacterially induced mineralization of calcium carbonate in terrestrial environments: the role of exopolysaccharides and amino acids. Journal of Sedimentary Research 73, 485-490.

Bristow, T. F., Milliken, R. E. (2011). Terrestrial perspective on authigenic clay mineral production in ancient Martian lakes. Clays and Clay Minerals, 59, 339-358.

Buczynski, C., Chafetz, H. S. (1993). Habit of bacterially induced precipitates of calcium carbonate: examples from laboratory experiments and recent sediments. In: Rezak, R., Lavoie, D. L. (Eds.). Carbonate Microfacies. Frontiers in Sedimentary Geology. pp 105-116.

Burne, R.V., Moore, L.S., Christy, A.G., Troitzsch, U., King, P.L., Carnerup, A.M. and Hamilton, P.J. (2014) Stevensite in the modern thrombolites of Lake Clifton, Western Australia: A missing link in microbialite mineralization? Geology 42, 575-578.

Calvo, J. P., Blanc-Valleron, M. M., Rodriguez-Arandia, J. P., Rouchy, J. M., Sanz, M. E. (1999). Authigenic clay minerals in continental evaporitic environments. In: M. Thiry and Simon-Coincon, R. (Eds.). Palaeoweathering, Palaeosurfaces and Related Continental Deposits. Special Publication of the International Association of Sedimentologists, 27, Blackwell Sciences, Oxford, UK. pp 129-151.

Chafetz, H. S., Butler, J. C. (1980). Petrology of recent caliche pisolites, spherulites, and speleothem deposits from Central Texas. Sedimentology, 27, 497-518.

Christensen, B.E. and Characklis, W.G. (1990) Physical and chemical properties of biofilms. Biofilms 93, 130.

Connell, T.L. and Dreiss, S.J. (1995) Chemical evolution of shallow groundwater along the northeast shore of Mono Lake, California. Water Resources Research 31, 3171-3182.

Della Porta, G. (2015). Carbonate build-ups in lacustrine, hydrothermal and fluvial settings: comparing depositional geometry, fabric types and geochemical signature. Geological Society, London, Special Publications, 418(1), 17-68.

Dittrich, M. and Sibler, S. (2010) Calcium carbonate precipitation by cyanobacterial polysaccarides, in: Pedley, H.M., Rogerson, M. (Eds.), Speleothems and Tufas: Unravelling Physical and Biological controls. Geological Society of London, London.

Dorobek, S., Piccoli, L., Coffey, B. and Adams, A. (2012). Carbonate Rock-Forming Processes in the Presalt "Sag" Successions of Campos Basin, Offshore Brazil: Evidence for Seasonal, Dominantly Abiotic Carbonate Precipitation, Substrate Controls, and Broader Geologic Implications. Abstract AAPG Hedberg Conference "Microbial Carbonate Reservoir Characterization" June 2012, Houston Texas.

Ercole, C., Bozzelli, P., Altieri, F., Cacchio, P., Del Gallo, M. (2012). Calcium carbonate mineralization: involvement of extracellular polymeric materials isolated from calcifying bacteria. Microscopy and Microanalysis, 18, 829-839.

Folk, R.L. (1974) The Natural History Of Crystalline Calcium Carbonate: Effect of Magnesium Content And Salinity. Journal of Sedimentary Petrology 44 40-53.

Hardalo, C. and Edberg, S.C. (1997) Pseudomonas aeruginosa: Assessment of Risk from Drinking Water. Critical Reviews in Microbiology 23, 47-75.

Humayoun, S. B., Bano, N., Hollibaugh, J. T. (2003). Depth Distribution of Microbial Diversity in Mono Lake, a Meromictic Soda Lake in California. Applied and Environmental Microbiology, 69 (2), 1030-1042.

Jones, B., Renaut, R. W. 1995. Noncrystallographic calcite dendrites from hot-spring deposits at Lake Bogoria, Kenya. Journal of Sedimentary Research, 64, 154-169.

Jones, B., Renaut, R. W. 1998. Origin of platy calcite crystals in hot-spring deposits of the Kenya Rift Valley. Journal of Sedimentary Research, 69, 913-926.

Jones, B. F., Deocampo, D. M. (2003). Geochemistry of Salines Lakes. In: J. J. Drever, D. H. Holland, and K.K. Turekian. (Eds.). Freswater Geochemistry, Weathering and Soils. Elsevier, New York, pp. 393-424.

Jones, B. and Peng, X. (2014) Signatures of biologically influenced CaCo3 and Mg–Fe silicate precipitation in hot springs: Case study from the Ruidian geothermal area, western Yunnan Province, China. Sedimentology 61, 56-89.

Kennedy, A.F. and Sutherland, I.W. (1987) Analysis of bacterial exopolysaccharides. Biotechnology and Applied Biochemistry 9, 12-19.

Kim, Y.-Y., Ganesan, K., Yang, P., Kulak, A.N., Borukhin, S., Pechook, S., Ribeiro, L., Kröger, R., Eichhorn, S.J., Armes, S.P., Pokroy, B. and Meldrum, F.C. (2011) An artificial biomineral formed by incorporation of copolymer micelles in calcite crystals. Nat Mater 10, 890-896.

Krause, S., Liebetrau, V., Gorb, S., Sánchez-Roman, M., McKenzie, J. A., Treude, T. (2012). Microbial nucleation of Mg-rich dolomite in exopolymeric substances under anoxic modern seawater salinity: New insight into an old enigma. Geology, 40, (7), 587-590.

Lopez-Garcia, P., Kazmierczak, J., Benzerara, K., Kempe, S., Guyot, F., Moreira, D. (2005). Bacterial diversity and carbonate precipitation in the giant microbialites from the highly alkaline Lake Van, Turkey. Extremophiles, 9 (4), 263-274.

Luiz Dias, J., 1998. Análise sedimentológica e estratigráfica do Andar aptiano em parte da margem leste do Brasil e no platô das Malvinas: considerações sobre as primeiras incursões e ingressões marinhas do oceano Atlântico Sul Meridional. Unpublished Ph.D. dissertation. Universidade Federal do Rio Grande do Sul. 1-411.

Meldrum, F.C. and Hyde, S.T. (2001) Morphological influence of magnesium and organic additives on the precipitation of calcite. Journal of Crystal Growth 231, 544-558.

McGill, R. A. R., Hall, A. J., Fallick, A. E., Boyce, A. J. 1993. The palaeoenvironment of East Kirkton, West Lothian, Scotland: stable isotope evidence from silicates and sulphides. Transactions of the Royal Society of Edinburgh: Earth Sciences, 894, (3-4), 223-237.

Niedermayr, A., Köhler, S.J. and Dietzel, M. (2013) Impacts of aqueous carbonate accumulation rate, magnesium and polyaspartic acid on calcium carbonate formation (6–40 °C). Chemical Geology 340, 105-120.

Orme, C.A., Noy, A., Wierzbicki, A., McBride, M.T., Grantham, M., Teng, H.H., Dove, P.M. and DeYoreo, J.J. (2001) Formation of chiralmorphologies through selective binding of amino acids to calcite surface steps. Nature 411, 775-779.

Passow, U., Shipe, R. F., Murray, A., Pak, D. K., Brzezinski, M. A., and Alldredge, A. L. (2001). The origin of transparent exopolymer particles (TEP) and their role in the sedimentation of particulate matter. Continental Shelf Research, 21(4), 327-346.

Passow, U. (2002a). Production of transparent exopolymer particles (TEP) by phyto- and bacterioplankton. Marine Ecology Progress Series, 236, 1-12.

Passow, U. (2002b). Transparent exopolymer particles (TEP) in aquatic environments. Progress in Oceanography, 55, 287-333.

Pedley, H.M. (1994) Prokaryote-microphyte biofilms and tufas: a sedimentological perspective. Kaupia, Darmstader Betr. Naturgesh. 4, 45-60.

Pedley, H.M., Rogerson, M. and Middleton, R. (2009) The growth and morphology of freshwater calcite precipitates from in Vitro Mesocosm flume experiments; the case for biomediation. Sedimentology 56, , 511-527.

PerryIV, T.D., Cygan, R.T. and Mitchell, R. (2006) Molecular models of alginic acid: Interactions with calcium ions and calcite surfaces. Geochimica et Cosmochimica Acta 70, 3508-3532.

Rees, H. C., Grant, W. D., Jones, B. E., Heaphy S. (2004). Diversity of Kenyan soda lake alkaliphiles assessed by molecular methods. Extremophiles, 8(1), 63-71.

Renaut, R. W., Owen, R. B., Jones, B., Tiercelin, J-J., Tarits, C., Ego, J. K., Konhauser, K. O. 2013. Impact of lake-level changes on the formation of thermogene travertine in continental rifts: evidence from Lake Bogoria, Kenya Rift Valley. Sedimentology, 60, 428-468.

Rodriguez-Navarro, C., Jimenez-Lopez, C., Rodriguez-Navarro, A., Gonzalez-Munoz, M-T., Rodriguez-Gallego, M. (2007). Bacterially mediated mineralization of vaterite. Geochimica et Cosmochimica Acta, 71, 1197-1213.

Rogerson, M., Pedley, H., Kelham, A. and Wadhawan, J. (2014) Linking mineralisation process and sedimentary product in terrestrial carbonates using a solution thermodynamic approach. Earth Surface Dynamics 2, 197-216.

Rogerson, M., Pedley, H.M. and Middleton, R. (2010) Microbial Influence on Macroenvironment Chemical Conditions in Alkaline (Tufa) Streams; Perspectives from In Vitro Experiments, in: Pedley, H.M., Rogerson, M. (Eds.), Speleothems and Tufas: Unravelling Physical and Biological controls. Geological Society of London, London, pp. 65-81.

Rogerson, M., Pedley, H.M., Wadhawan, J.D. and Middleton, R. (2008) New Insights into Biological Influence on the Geochemistry of Freshwater Carbonate Deposits. Geochimica et Cosmochimica Acta 72, 4976-4987.

Saiz-Jiménez, C. (1999) Biogeochemistry of weathering processes in monuments. Journal of Geomicrobiology 16, 27-37.

Sánchez-Navas, A., Martin-Algarra, A., Sánchez-Roman, M., Jiménez-López, C., Nieto, F., Ruiz-Bustos, A. (2013). Crystal growth of inorganic and biomediated carbonates and phosphates. Advanced Topics on Crystal Growth. pp. 1-22.

Sánchez-Navas, A., Martín-Algarra, A., Rivadeneyra, M. A., Melchor, S. Martín-Ramos, J-D. (2009). Crystal-growth behaviour in Ca-Mg carbonate bacterial spherulites. Crystal Growth and Design, 9, (6), 2690-2699.

Saunders, P., Rogerson, M., Wadhawan, J., Greenway, G. and Pedley, H. (2014) Mg/Ca ratios in freshwater microbial carbonates: Thermodynamic, Kinetic and Vital Effects. Geochimica et Cosmochimica Acta.

Schwarz, K. (1973) A Bound Form of Silicon in Glycosaminoglycans and Polyuronides. Proceedings of the National Academy of Sciences 70, 1608-1612.

Spadafora, A., Peri, E., McKenzie, J. A., Vasconcelos, C. (2010). Microbial biomineralization processes forming modern Ca:Mg carbonate stromatolites. Sedimentology, 57 (1), 27-40.

Sunagawa, I. (2005). Crystals: growth, morphology, & perfection. Cambridge University Press.

Sychev, M., Prihod'ko, R., Koryabkina, A., Hensen, E.J.M., van Veen, J.A.R. and van Santen, R.A. (2000) The application of non-hydrothermally prepared stevensites as support for hydrodesulfurization catalysts, in: E.

Gaigneaux, D.E.D.V.P.G.P.A.J.J.A.M.P.R., Poncelet, G. (Eds.), Studies in Surface Science and Catalysis. Elsevier, pp. 257-265.

Terra et al., 2010. Classificação de rochas carbonáticas aplicável às bacias sedimentares brasileiras. Bulletin Geoscience Petrobras, Rio de Janeiro, 18 (1), 9-29.

Tosca, N. J., Masterton, A. L. (2014). Chemical controls on incipient Mg-silicate crystallisation at 25°C: implications for early and late diagenesis. Clay Minerals, 49, 165-194.

Tosca, N. J., & Wright, V. P. (2015). Diagenetic pathways linked to labile Mg-clays in lacustrine carbonate reservoirs: a model for the origin of secondary porosity in the Cretaceous pre-salt Barra Velha Formation, offshore Brazil. Geological Society, London, Special Publications, 435, SP435-1.

Tourney, J., Ngwenya, B. T. (2009). Bacterial extracellular polymeric substances (EPS) mediate CaCO3 morphology and polymorphism. Chemical Geology, 262, 138-146.

Tracey, S. L., François, C. J. P., Jennings, H. M. (1998). The growth of calcite spherulites from solution I. Experimental design techniques. Journal of Crystal Growth, 193, 374-381.

Tracey, S. L., Williams, D. A., Jennings, H. M. (1998). The growth of calcite spherulites from solution II. Kinetics of formation. Journal of Crystal Growth, 193, 382-388.

Verrecchia, E. P., Freytet, P., Verrecchia, K. E., Dumont, J-L. (1995). Spherulites in calcrete laminar crusts: biogenic CaCO3 precipitation as a major contributor to crust formation. Journal of Sedimentary Research, 65A (4), 690-700.

Wanas, H. A. (2012). Pseudospherulitic fibrous calcite from the Quaternary shallow lacustrine carbonates of the Farafra Oasis, Western Desert, Egypt: a primary precipitate with possible bacterial influence. Journal of African Earth Sciences, 65, 105-114.

Wolthers, M., Nehrke, G., Fokkema, M. (2008). Coupled effects of aspartic acid and magnesium on biocalcification. Geophysical Research Abstr., EGU General Assembly.

Wright, V. P. 2012. Lacustrine carbonates in rift settings: the interaction of volcanic and microbial processes on carbonate deposition. Geological Society, London, Special Publications 2012, 370, 39-47.

Wright, V. P., Barnett, A. J. (2015). An abiotic model for the development of textures in some South Atlantic early Cretaceous lacustrine carbonates. In: Bosence, D. W. J., Gibbons, K. A., le Heron, D. P., Morgan, W. A., Pritchard, T. & Vining, B. A. (eds). Microbial Carbonates in Space and Time: Implications for Global Exploration and Production. Geological Society, London, Special Publications 418, 209-219.

FIGURE CAPTIONS

TABLE 1. Initial composition of solution used in experiments

FIGURE 1. Crystals precipitated in the control experiment. (A) Subhedral to euhedral calcite crystals (EDX spot analysis on asterisk indicate calcium carbonate composition). (B) Detail of A with composite rare spherulites made up of rhombic and trigonal bladed calcite imbricated crystals. (C) Abundant subhedral to euhedral halite cubic crystals (Na).

(D) Halite crusts developing chevron overgrowth crystals (EDX spot analysis on asterisk indicate sodium chloride composition).

FIGURE 2. Crystals precipitated in the presence of alginates. (A) Calcitic spheroidal clusters attached to the glass slide. (B) Spherulitic particles are made up of imbricated rhombohedron twins (up to 10µm diameter each). Partial aggregation and fusion of spherulitic components is observed (arrow). (C) Broken spheres display hollow centres. (D) Distinctive subhedral to mainly euhedral botryoidal crusts (arrow) nucleate above previous spherulitic after 44 days.

FIGURE 3. X-ray powder diffraction pattern of spherulitic components. The lower set of lines indicates the expected peak positions and approximate intensities for a pure sample of calcite.

FIGURE 4. Crystals precipitated in presence of sodium carboxymethil cellulose. (A) Euhedral sheets of well-formed calcite rhombohedrons (EDX spot analysis on asterisk indicate calcium carbonate composition). (B) Calcite spherical particles growing intertwined with calcite rhombohedrons. (C) Thin calcite crusts (bottom right) formed by nanometre-thick spheroidal calcite aggregates give rise to spherical particles up to 10µm in diameter. (D) Elongated hollow spheres (up to 3 µm in diameter) forming cluster aggregates intermingled with calcite rhombohedrons.

FIGURE 5. Crystals precipitated in presence of stevensite. (A) Euhedral needle-like calcite crystals (Cal) exhibit inter-grown twinning (arrow), and are intermingled with subhedral to poorly developed stevensite crystals (St). (B) Detail of the needle to sheet-like elongated

rhombohedral calcite bouquets. Some calcite crystals (arrows) show earlier growth stages and poorly developed and tiny stevensite crystals (St) appear in the background. (C) Subhedral to amorphous stevensite crystals (EDX spot analysis on asterisk indicates stevensite composition) intermingled with needle-like subhedral calcite crystals (Cal). (D) Macroscopic (mm-sized) stevensite crystals accumulated in the bottom of the flasks (EDX spot analysis on asterisk indicates stevensite composition).

FIGURE 6. Crystals precipitated in presence of stevensite and alginates. (A) Tiny, anhedral calcite precipitates (Cal) and dispersed and small aggregates of Mg-hydrated magnesium clays (St). (B) Abundant stevensite clay patchy crystals (EDX spot analysis on asterisk indicate stevensite composition) intermingled with some prismatic and elongated calcite precipitates (top right) and small cubic aggregates of sodium chloride crystals (Na). (C) Poorly defined, anhedral stevensite crystals (St) surrounded by sub-cubic aggregates of sodium chloride crystals (Na). (D) Mm-sized stevensite crystals accumulated in the bottom of the flasks (EDX spot analysis on asterisk indicate stevensite composition).

FIGURE 7. Calcium loss from solution during experiments, given in mg day-1. Filled circles are 24 days, open circles are 37 days and triangles are 45 days.

FIGURE 8. Magnesium loss from solution during experiments, given in mg day-1. Filled circles are 24 days, open circles are 37 days and triangles are 45 days. Note negative values indicate an increase in concentration.

FIGURE 9. Silicon loss from solution during experiments, given in mg day-1. Filled circles are 24 days, open circles are 37 days and triangles are 45 days. Note negative values indicate an increase in concentration.

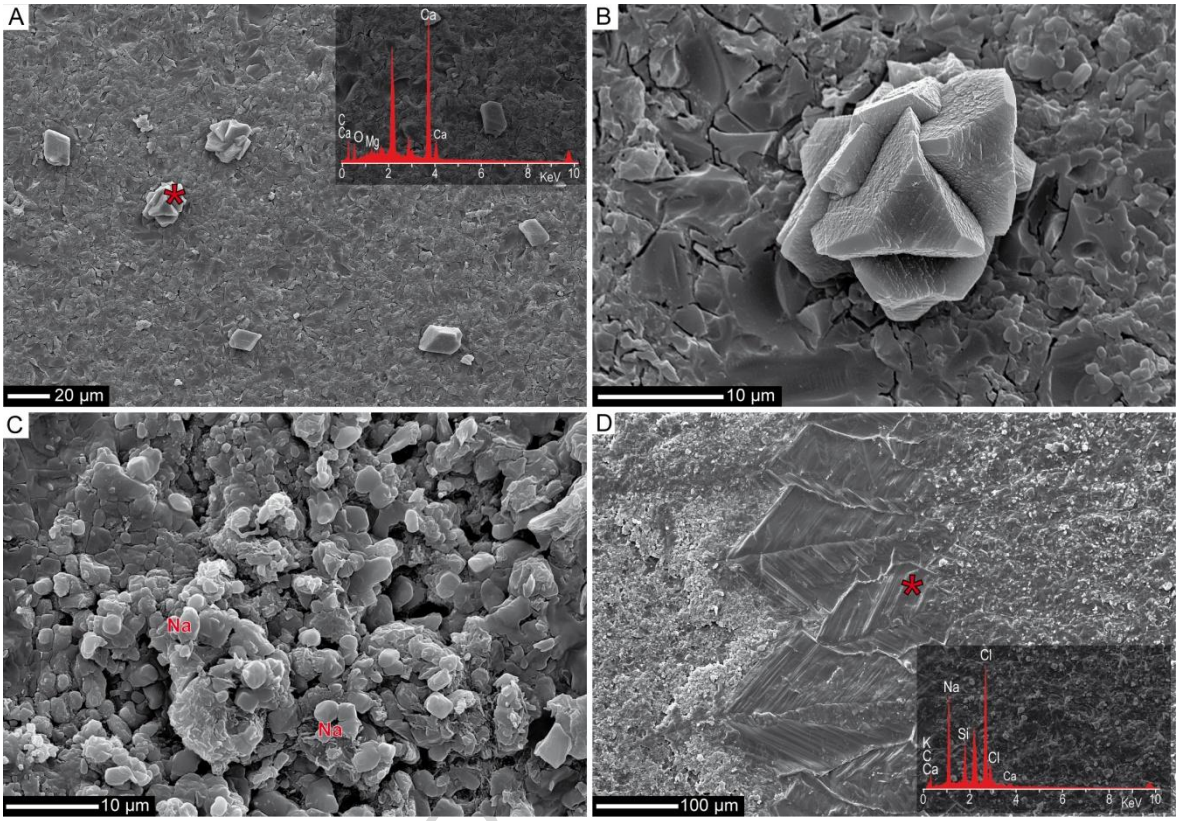

Figure 1

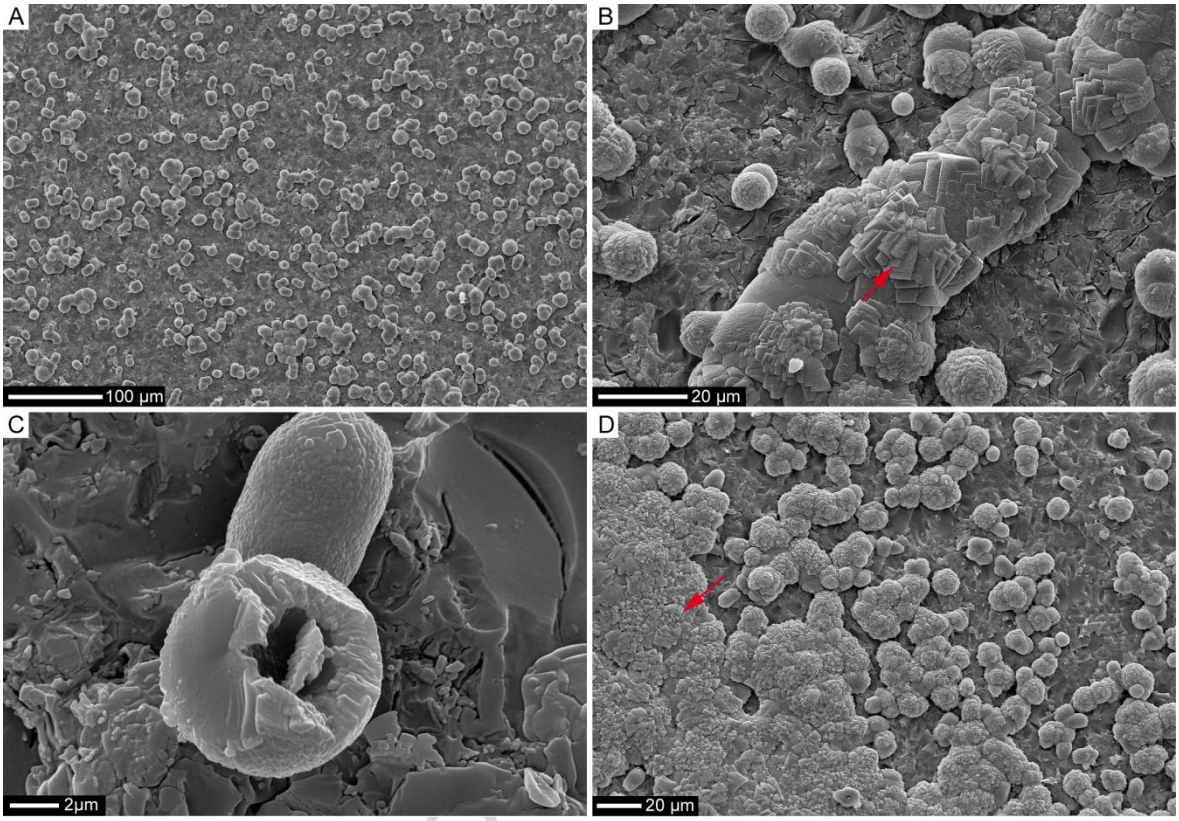

Figure 2

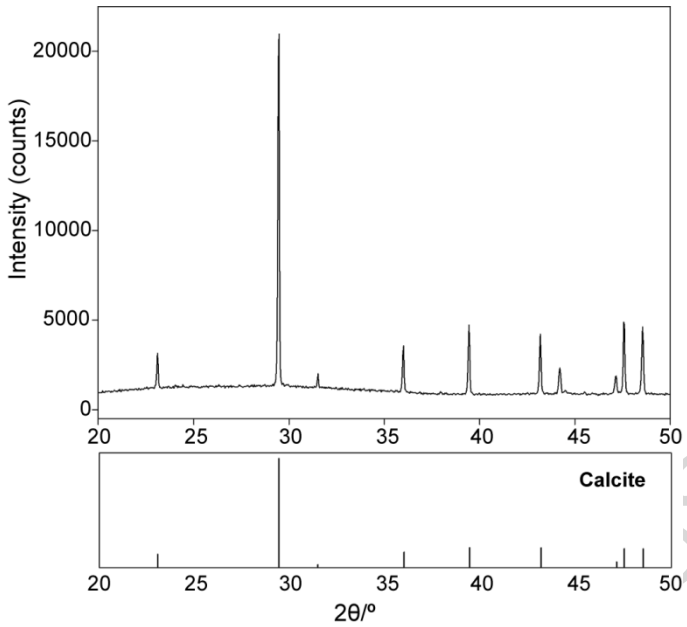

Figure 3

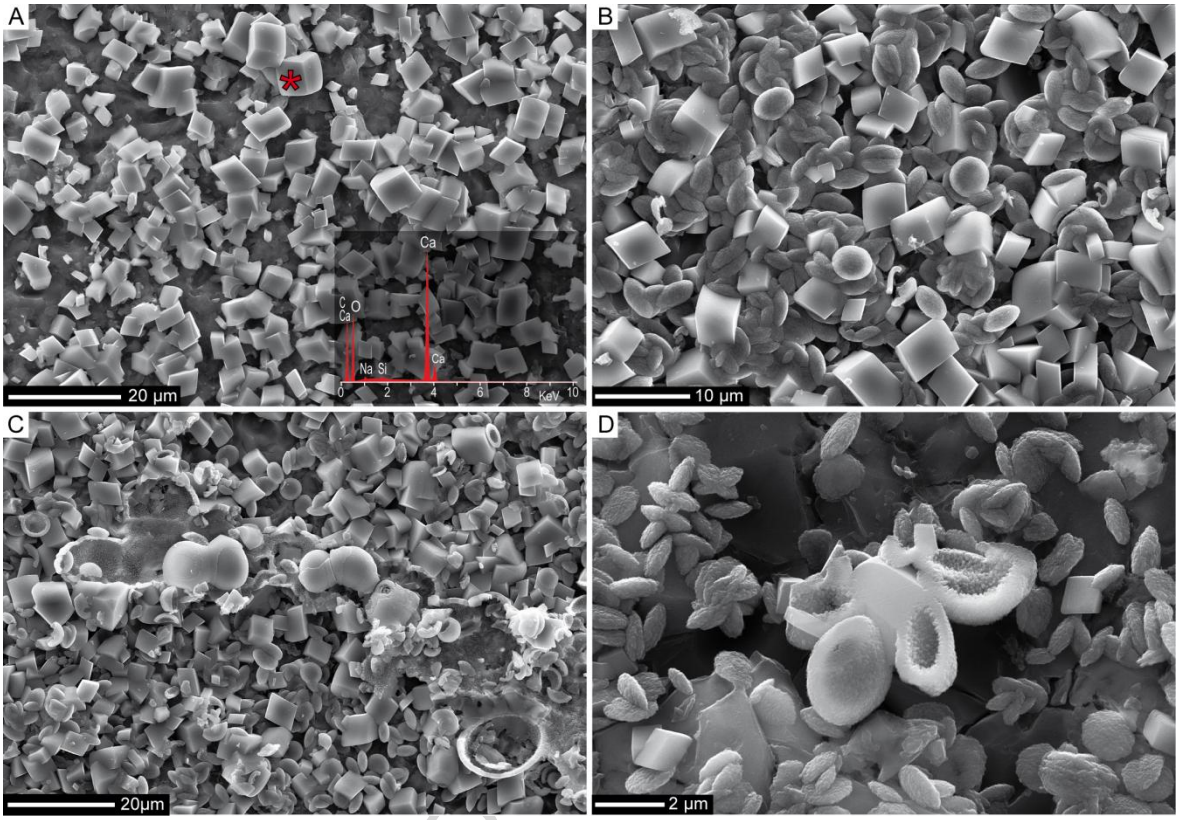

Figure 4

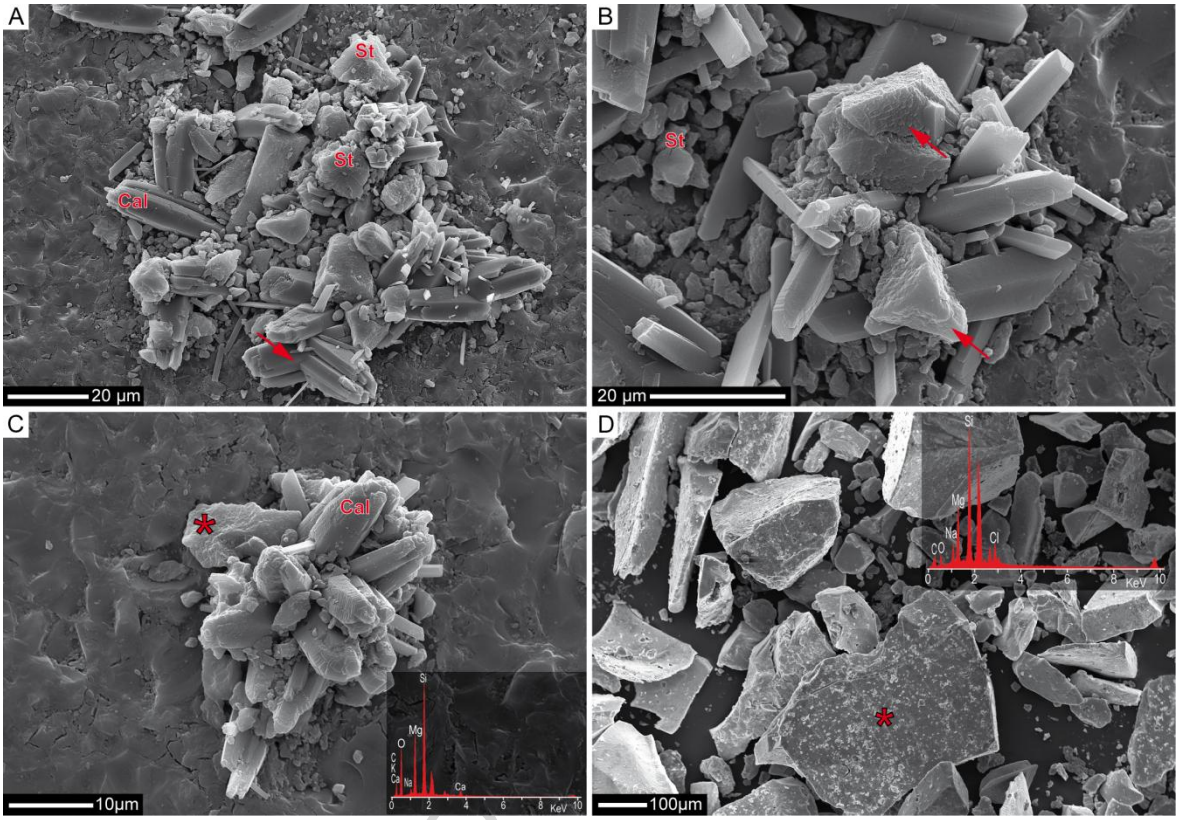

Figure 5

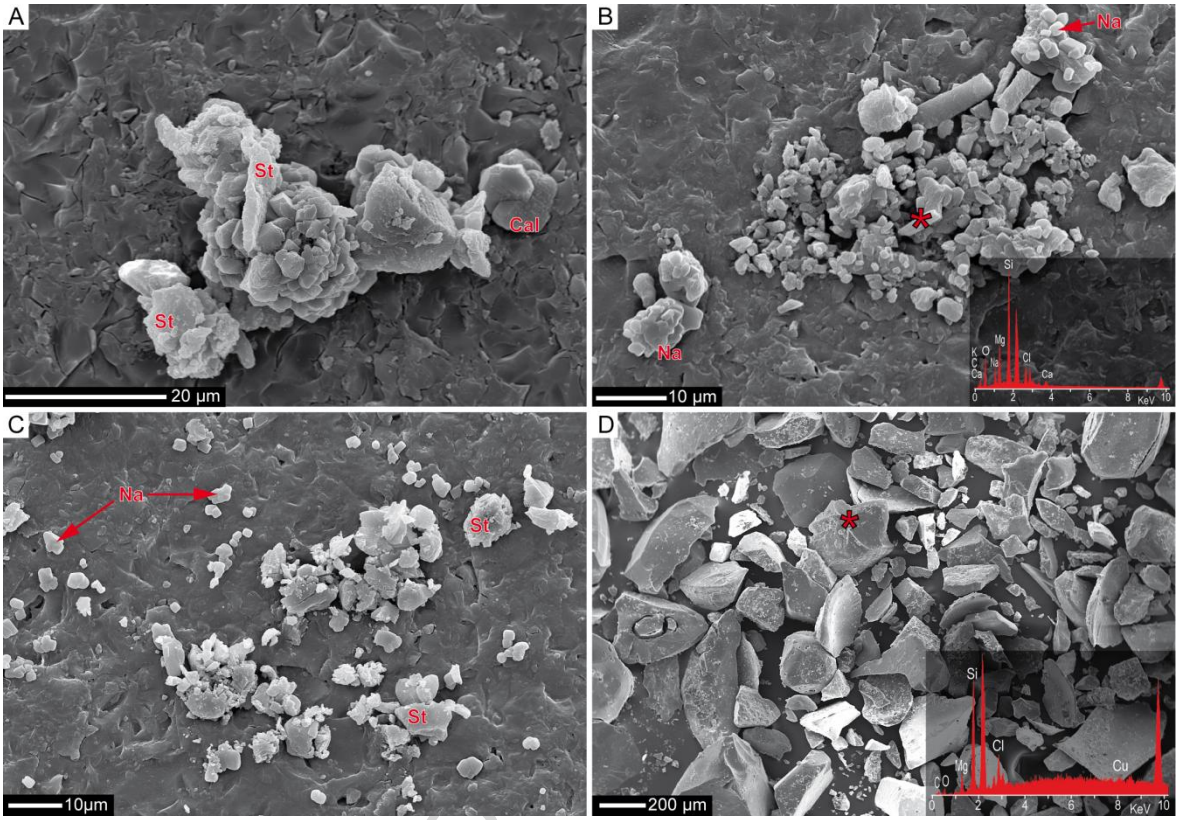

Figure 6

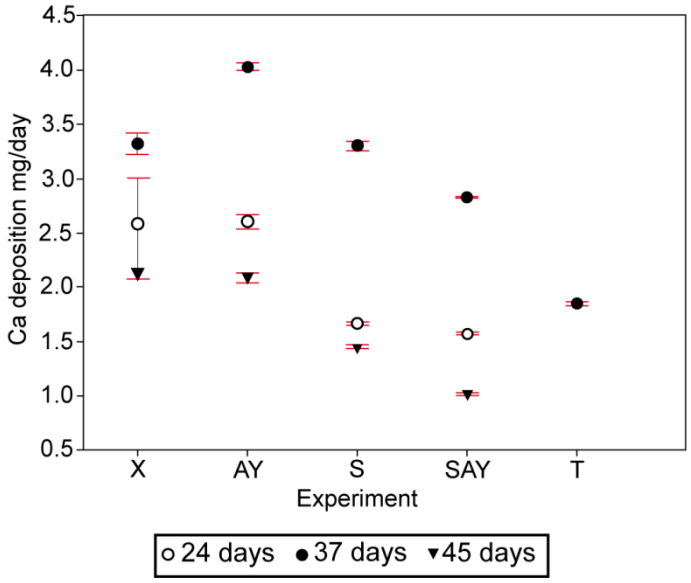

Figure 7

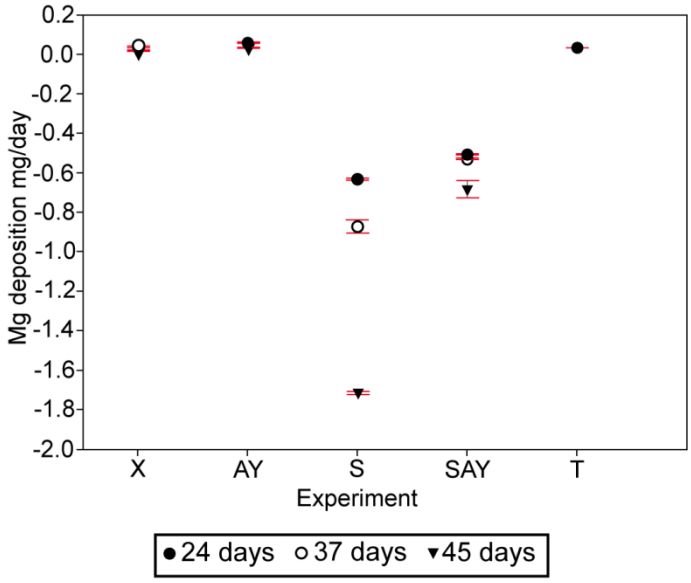

Figure 8

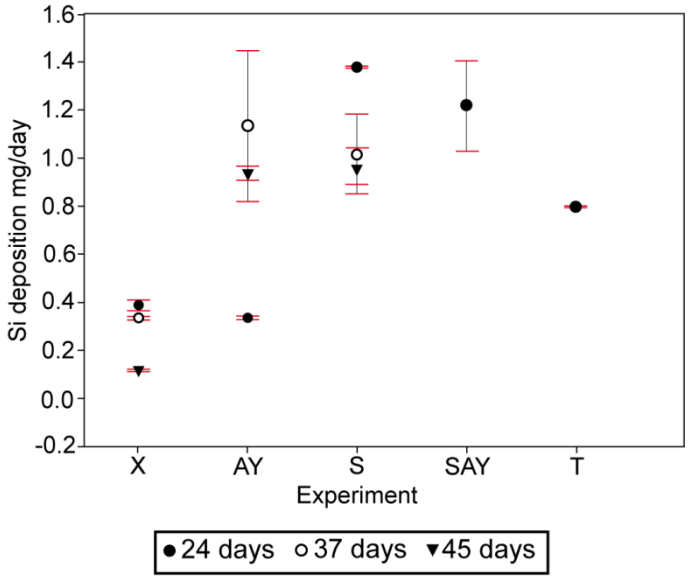

Figure 9

Element	mg/L
Cl	10930
Na	6716
K	682
Mg	125
Ca	162
Si	17
Alkalinity	299.7 meq
Saturation Index	1.65

Table 1.

Highlights

A sterile solution replicating Mono Lake waters was used in this experimental study

Spherulitic calcite formed within a saline, alkaline water rich in organic acids

Calcite precipitation rate increased under the presence of diverse organic molecules

Calcite precipitation rate decreased when solution was supersaturated in stevensite

Spherulitic calcite did not form when solution was supersaturated in stevensite